Stabilization of defects by the presence of hydrogen in tungsten: simultaneous W-ion damaging and D-atom exposure

E.A. Hodille, S. Markelj, T. Schwarz-Selinger, A. Založnik, M. Pečovnik, M. Kelemen, C. Grisolia

Stabilization of defects by the presence of hydrogen in tungsten: simultaneous W-ion damaging and D-atom exposure

E. A. Hodille[e], S. Markelj[*a], T. Schwarz-Selinger[c], A. Založnik[a], M. Pečovnik, M. Kelemen[a,d], C Grisolia[c]

[a]*Jožef Stefan Institute, Jamova cesta 39, 1000 Ljubljana, Slovenia*
[b]*CEA, IRFM, F-13108 Saint Paul Lez Durance, France*
[c]*Max-Planck-Institut für Plasmaphysik, Boltzmannstrasse 2, D-85748 Garching, Germany*
[d]*Jozef Stefan International Postgraduate School, Jamova cesta 39, 1000 Ljubljana, Slovenia*
[e]*Department of Physics, University of Helsinki, P. O. Box 43, FI-00014, Finland*

Abstract

The possible synergistic effect and mutual influence of the defect production by W-ion damaging and presence of hydrogen isotopes in the crystal lattice of tungsten is studied. For this purpose we perform modelling of the experimental data where samples were in one case sequentially damaged by W ions followed by D-atom exposure and in the other case simultaneously damaged by W ions and exposed to D atoms. Modeling is performed by the MHIMS (migration of hydrogen isotopes in materials) code in which a model of trap creation due to W-ion irradiation during the D-atom exposures is implemented. With the help of the surface model and the experimental data the migration barrier from the surface to the bulk is determined as a function of exposure temperature. It is shown that there is a temperature dependence of the migration barrier which at high temperatures and low hydrogen atom surface coverages stabilizes at 2 eV being in good agreement with the first-principle calculations. The evolution of trap concentrations with temperature is obtained from fitting the deuterium (D) depth profiles and the thermo-desorption spectra of deuterium gas at different damaging temperatures. In both experiments, the desorption peaks corresponding to induced trap defects are described by two trapping types with energies of 1.83 eV and 2.10 eV attributed to dislocation loops and cavities, respectively. The concentration of the low energy trap is higher in the case of simultaneous W/D exposure as compared to sequential W/D exposure experiment. This gives an unambiguous proof that the presence of deuterium does have an influence of defect evolution in tungsten material and therefore prevents spontaneous annihilation the traps.

[*]Corresponding author: sabina.markelj@ijs.si

1. Introduction

Hydrogen interaction with materials plays a crucial role in fusion research as the tritium inventory needs to be controlled inside a future reactor and maintained below specific limits for safe and fuel-efficient operation. Current fusion development concepts aim to produce energy in a closed tritium fuel cycle [1]. Moreover fusion reactor like DEMO needs to have materials that operate at elevated temperatures (< 1500 K) and withstand intense heat loads up to 10 MW/m^2 and large particle fluxes up to 10^{24} part/m^{2}s [2]. Within expected operational duty cycles the displacement damage from irradiation by energetic 14.1 MeV neutrons produced by the deuterium-tritium fusion reaction (D + T → He (3.5 MeV) + neutron (14.1 MeV)) is anticipated to be few displacements per atom per year [3], adding additional challenges to material choices. Based on these considerations, tungsten (W) and tungsten-based alloys have been proposed as materials to be used as plasma facing components. Therefore, we need to be able to predict the hydrogen isotope (HI) inventory in tungsten under the harsh conditions taking place in a future fusion reactor, necessarily taking into account also the effect of neutrons. Lattice defects induced by neutron irradiation act as trapping sites for HIs characterized by high de-trapping energy as compared to the energy of diffusion between solute interstitial sites. These traps have a strong impact on the overall tritium retention as predicted by rate equation simulations of tritium retention in W during realistic tokamak cycles [4]. During fusion reactor plasma operation both implantation of energetic hydrogen isotope ions and neutrals as well as damage creation by neutron irradiation will take place at the same time. The consequences of simultaneous/mutual influence on defect structure and fuel retention is still not well understood. Dedicated experiments as well as theory are needed to address these extreme conditions [5, 6]. However, there is currently no facility capable of replicating the extreme operating environments of high particle and heat fluxes, large time-varying stresses, and large fluence of 14.1 MeV fusion neutrons [5]. Therefore, well-defined laboratory experiments are needed for validation of models in order to understand the basic processes, such as HIs transport in a material with induced lattice defects, the effect of HI and impurity atoms on defects evolution and the role of the surface on HIs absorption and desorption. For this purpose, benchmark experiments are needed where D atoms are a convenient tool to detect and describe the nature of defects: their de-trapping energy for HI and evolution with sample temperature with and without the presence of HI. Computational simulations of such well-defined experiments can then provide extrapolations from validated cases to extreme environments that remain inaccessible experimentally, giving qualitative and quantitative insights into material evolution and properties.

To study the influence of material displacement damage on fuel retention, high energy ions are used [7] as a surrogate for the displacement damage that neutron irradiation will cause. It has been shown that fuel retention both in fission neutron-damaged [8] and in W-ion-damaged tungsten (so-called self-damaged W) is strongly increased as compared to undamaged tungsten (e.g. [9, 10]).

In this paper we model the experimental results presented in [11] using the code MHIMS solving a set of rate equations. Namely, simultaneous W-ion irradiation and D-atom exposure at different

2

elevated temperatures are performed and compared to the results of sequential procedure of W-ion damaging at elevated temperatures and D-atom exposure. In order to obtain a deeper insight into the evolution of individual traps with damaging temperature thermal desorption spectroscopy (TDS) was performed on those samples providing us the information on the evolution of the desorption spectra with the experimental procedure and therefore indication on the behavior of individual traps. A combination of modeling the TDS spectra and D depth profiles shown in [11] gave us the possibility to study the influence of deuterium presence on evolution of individual trap with temperature.

2. Experiment

The details of the simultaneous W-ion damaging and D-atom exposure experiments were already given in [11]. Still a short overview of the experimental procedure and conditions will be given. Polycrystalline 99.997 wt. % hot-rolled tungsten samples (PW) were used in the present experiment. Samples were recrystallized before the experiment to enlarge grain size to about 50 μm and to reduce the natural defects present in the samples.

In order to study the effect of HI presence in the material on damaging two experimental procedures were used: *sequential W-ion damaging at elevated temperatures and D-atom exposure* (in short: sequential W/D exposure) and *simultaneous W-ion irradiation and D-atom exposure* (in short: simultaneous W/D exposure). In the first case the samples were first damaged at different sample temperatures by 10.8 MeV W^{6+} tungsten ions for four hours to a fluence of 1.4×10^{18} W/m^2 creating a damage dose of 0.47 dpa_{KP} at the peak maximum (calculated by SRIM program with Kinchin-Pease calculation, 90 eV displacement damage energy, evaluating the "vacancy.txt" output). This yields a displacement rate of 3.3×10^{-5} dpa/s. The damaging temperatures are 300 K, 600 K, 800 K and 1000 K. After damaging, the samples were exposed for 24 h to D atoms of 0.28 eV with flux density of 5.4×10^{18} $D/m^2 s$, fluence of 4.7×10^{23} D/m^2 at 600 K sample temperature. The exposure to D atoms is a tool to populate the traps created in the sample and from D retention and desorption deduce the traps concentrations and de-trapping energies. Exposure to D atoms is the most gentle way of hydrogen isotope exposure not producing any additional damage. The data from sequential damaging experiment at 300 K can be compared to our previous studies with self-damaged W in order to check the damaging procedure and reproducibility of D-atom exposure with respect to the maximum D concentration [12, 13]. The agreement is very good. In the case of the second experimental procedure *simultaneous W-ion damaging and D-atom exposure* the samples were damaged with the same energy and flux as in the case of *sequential damaging at elevated temperature and D-atom exposure.* In addition, during the damaging procedure, the samples were also exposed to a beam of neutral D atoms with 0.28 eV and flux density of 5.4×10^{18} $D/m^2 s$ at the probing ion beam position. The simultaneous

experiment was performed at five different temperatures of 450 K, 600 K, 800 K, 900K and 1000 K. The D-atom exposure started 20 min before the beginning of the W-ion irradiation. After the end of the W-ion irradiation the sample heating was first stopped. D exposure was ended only when the sample temperature was at least 100 K below the exposure temperature to avoid thermal losses of D. Since the temperature influences the final D atom depth distribution in the material, we will specify for individual exposures at which temperature the D atom exposure was terminated. Namely, the D-atom exposures were stopped after approximately 3 min at 423 K sample temperature in the 450 K case, at 488 K for the 600 K case, at 612 K for the 800 K, at 693 K for the 900 K and at 753 K for the 1000 K. After four hours of damaging the deuterium depth profiles were measured by nuclear reaction analysis (NRA) utilizing ^{3}He beam. The D depth profile analysis was performed at the central position of the W irradiation beam. The ^{3}He analyzing beam was 2 mm in diameter which is smaller compared to the size of the W ion beam being 4 mm in diameter. After the D depth profile analysis, the samples were again exposed to D atoms at 600 K sample temperature for 19 hours yielding a fluence of 3.7×10^{23} D/m^2. The purpose of this additional exposure was again to use the D retention (defect population by D atoms) to compare the quantity of defects actually created in the material during the simultaneous W-ion irradiation and D-atom exposure. Namely, the depth profiles obtained after the first 4 hours give us only the information on how deep the atoms penetrated during the simultaneous W-ion irradiation and D-exposure. The D retention in this case does not give us the information about trap concentration, since the D atom fraction changes strongly with the exposure temperature. The higher the temperature, the more efficient is the D-atom de-trapping. In addition, the additional 19 hours exposure to D atoms at 600 K sample temperature allows us to directly compare the depth profiles and the maximum D-atom concentration in the material at the maximum of damage dose for both experiments. As was shown in [11] (figure 6) the simultaneous experiment yields about a factor of 1.3 higher maximum D concentration as compared with sequential damaging at elevated temperatures in the range from 600 K to 1000 K. In addition, the behavior is different at temperatures above 800 K. For the simultaneous W/D exposure D retention saturates at temperatures ≥900 K. To recheck the phenomenon of D atom concentration stabilization above 900 K the simultaneous W-ion irradiation and D-atom exposure was repeated at 1000 K and extended to 1130 K sample temperature. In this case the W ion flux was two times higher and hence the exposure time was adjusted to half the time to reach the same final damage dose of 0.47 dpa$_{KP}$.

After the NRA analysis at JSI the samples were analyzed at IPP, Garching with NRA for deuterium signal profile along the sample giving us information about W beam diameter and homogeneity. After this analysis, TDS was performed on the samples, where the samples were heated in the TESS set-up at IPP with a linear temperature ramp of 15 K/min up to 1323 K and held at the highest temperature for 5 min. The calibration of D$_2$ detection sensitivity of the mass spectrometer was performed by a D$_2$ calibration Laco gas bottle with calibrated leak rate of 1.2234×10^{14} D$_2$ molecules/sec [14].

3. Simulations

To simulate the simultaneous W-ion irradiation and D-atom exposure, we employed the MHIMS code [15], using the surface model [16] developed to handle low energy hydrogen atom exposures. This code is based on 1D macroscopic rate equation (MRE) model widely used to tackle implantation and desorption of hydrogen isotopes in W like in TMAP7 code [17] or TESSIM code [18, 19]. The model implemented in MHIMS as well as its parameters are reported in table 1 of [16]. The MHIMS free parameters are the energies at the surface (desorption energy E_D, surface to bulk energy E_A, bulk to surface energy E_R), the detrapping energies $E_{t,i}$ of the traps created by W damaging and their concentrations n_i (m^{-3}). In the case of simultaneous W damaging and D exposure, these traps are initially absent in the material and are created during W irradiation of the material. To simulate this dynamical creation of traps, a creation model has been implemented in MHIMS for the self-damaged traps. This model has a similar formalism as the one proposed by Ogorodnikova et al. [20] to simulate ion-induced traps: if one calls n_i the concentration of self-damaged trap type i (in m^{-3}) characterized by a trapping energy $E_{t,i}$, its evolution with time is given by equation (1).

$$\frac{dn_i}{dt} = \varphi_W \left(f(x) - \frac{n_i}{n_{i,max}} \right) \eta_i \qquad (1)$$

where

- φ_W ($m^{-2}s^{-1}$) is the implantation flux of W ions that damage the material,
- $n_{i,max}$ (m^{-3}) is the maximum concentration of self-damaged trap of type i,
- η_i (m^{-1}) is the creation rate of traps
- $f(x)$ (dimensionless) is the depth (x) distribution of the created traps.

The steady state of this equation gives a depth distribution of the self-damaged traps as $n_i = n_{i,max}f(x)$. No damage is induced deeper than 1.5 µm which is the range of the damaging zone for 10.8 MeV W ions [11]. Thus, we choose $f(x)$ as shown in figure 1 to reproduce this feature. The maximum value of $f(x)$ is 1 meaning that $n_{i,max}$ represents the maximum of the concentration of self-damage trap i.
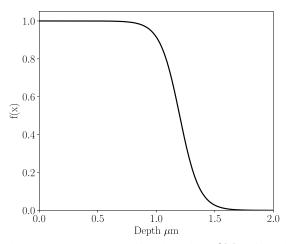
Figure 1. Creation distribution f(x) of self-damaged traps.

A saturation limit of created defects is used since it was observed experimentally in several publications [21, 22, 10] that there is a saturation of D retention for W fluence above 3×10^{17} Wm^{-2} (~0.2 dpa with 12.3 MeV/W and 20 MeV). In the experiments simulated in this paper, the W fluence is much higher (1.4×10^{18} Wm^{-2}) than the W fluence needed for D saturation assuming that the experimental saturation limit is 3×10^{17} Wm^{-2}. Thus, it is most likely that the concentrations of self-damaged traps are saturated in the damaged zone. In the current creation model, this saturation is expressed by $n_{i,max}$. In the simple current model, for a constant flux φ_W, the concentration of created traps evolves with the W fluence Φ_W as follows: $n_i(\Phi_W, x) = f(x) n_{i,sat}\left(1 - \exp\left(-\frac{\Phi_W}{\Phi_W^i}\right)\right)$ with $\Phi_W^i = \frac{n_{i,max}}{\eta_i}$ (Wm^{-2}) the characteristic W fluence governing the growth of n_i. For $\Phi_W = 3\Phi_W^i$, $n_i = 0.95 n_{i,max}$ meaning that it can be considered as saturated. To determine the value of η_i, one can extract the evolution of the D retained in each trap by simulating TDS/depth profile obtained for various low fluences (to be sure to be outside of the fluence range where there is a saturation of the concentrations of traps). Taking the saturation fluence determined by 't Hoen et al., one obtains $\eta_i \approx \frac{5 \times 10^2}{\int f(x)dx}$ for all self-damaged traps and all irradiation temperatures (it means that each W ion would create 5×10^2 traps in the damaged zone f(x)). It has to be noted here that the saturation limit might be different for simultaneous W/D exposure and depends especially on the concentration of hydrogen inserted in the materials. However, its determination would require supplementary experimental data (retention with W fluence during simultaneous exposure) and the scope of this article is more focused on the determination of the maximal quantity of trap $n_{i,max}$ when the concentrations of self-damaged traps are saturated. Finally, at a fluence of 1.4×10^{18} Wm^{-2} with such distribution and value of η_i, the final self-damaged trap concentrations are constant and equal to $n_{i,max}$ (given in table 1) near the surface and then smoothly decrease to zero between 1.0 and 1.5 μm.

6

The simulated experiment can be divided into three main steps corresponding to different experimental procedures:

- A simultaneous D/W exposure (at 450 K, 600K, 800 K, 900 K or 1000 K) for 4 hours and cooling down to room temperature. The atom flux is $\Gamma_{atom} = 5.4 \times 10^{18}$ m^{-2}s^{-1}. The flux of W ions is $\varphi_W = 9.7 \times 10^{13}$ Wm^{-2}s^{-1}.

- A D-atom exposure at 600 K for 19 hours. The atom flux is the same as in the first phase of the experiment.

- A TDS with a heating ramp of 15 K/min.

Between two different steps, a "storage" phase (e.g. no exposure flux and constant temperature) is simulated that lasts several thousands of seconds so the system evolves to a realistic kinetic equilibrium where the mobile and weakly bonded particles are removed from the system before any TDS or re-exposure. These storage phases are done at 300 K. The temperature is cooled down to 300 K with the same evolution as in the experiments. It is particularly important to simulate the correct decrease of sample temperature after the simultaneous D/W exposure, as the flux of D atoms is switched off about 3 minutes after the decrease of the temperature. As it will be explained in the following, this delay could induce increase of the deuterium concentration in the first hundreds of nanometers observed in the experiments just after the simultaneous exposures (figure 4).

In addition to the simulation of simultaneous exposure followed by a re-exposure to D atoms and a TDS phase, simulations of sequential W damaging at different temperatures and D-atom exposure for 24 h at 600 K, $\Gamma_{atom} = 5.4 \times 10^{18}$ m^{-2}s^{-1} and TDS sequences will be also presented. In both damaging experiments 10.8 MeV W ions are used with the same dose. Thus, the distribution of self-damaged traps in both sets of simulations are the same (figure 1). Consequently, if one observes a difference in terms of trap nature or trap concentration, this would only be due to the influence of deuterium during the trap creation processes.

3.1 Surface modelling and associated E_D and E_A energies

Let us detail the surface modelling used in the MHIMS code.

Denoting n_{surf} (m^{-2}) the concentration of surface site and c_{surf} (m^{-2}) the concentration of hydrogen atom on the surface one can define the coverage as $\theta = c_{surf}/n_{surf}$. Its highest value is 1.

The free parameters of the surface model are the surface desorption energy per D E_D (eV), the activation energy for absorption from the surface to the bulk E_A and the activation energy for E_R corresponding to the release of D atom from the bulk to the surface (called resurfacing in the following). We choose to use $E_R = 0.2$ eV which is the energy barrier for diffusion of interstitial site in W calculated by density functional theory calculations [23].

Previous MRE simulations of atomic exposure [16] showed that the surface energies, E_D (from the surface to the vacuum) and E_A (from the surface to the bulk), are dependent on the surface

conditions as suggested by DFT calculations [24, 25] and experimental measurements [26, 27]. This suggests the presence of different binding sites for HI on the W surface (with different desorption energies [26, 28]) that are progressively populated as the hydrogen atom coverage increases. Initially, in the MHIMS code, the interactions of hydrogen with the W surface was implemented for constant values of E_D and E_A since the simulated exposure were done at a given temperature. However, in the present simulations, the samples are exposed at different temperatures corresponding to different surface conditions. To take into account these effects, we decided to introduce coverage dependent surface energies $E_D(\theta)$ and $E_A(\theta)$. These evolutions are shown in figure 2.
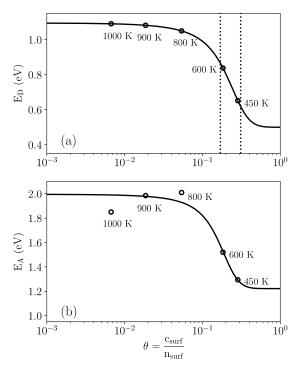

Figure 2. Evolution of the surface energies E_D (a) and E_A (b) with the coverage $\theta = c_{surf}/n_{surf}$. On (a), the open circles represent the value of E_D obtained from the simulation once the steady-state of θ is reached for the different exposure conditions. On (b), the open circles represent the value of E_A required to have a total simulated D concentration in the damaged layer equal to the experimental D concentration for the different exposure conditions.

First the evolution of E_D with the coverage (figure 2a) is determined. The energy reported in [16] ($E_D = 0.69 - 0.87$ eV) corresponding to MHIMS simulations of D atomic exposure at 500 K and 600 K are in good agreement with the one reported by Zaloznik et al. [19] ($E_D = 0.68$ eV $- 0.71$ eV) from TESSIM simulations of a similar experiment: D-atom exposure at temperatures from 450 K to 600 K. Markelj et al. [28] reported 3 adsorption sites on the surface with desorption energies ($2E_D$) of 1.05 eV, 1.64-1.7 eV and 2.2 eV with respective concentrations of 5×10^{19}, 1.0×10^{19} and 1.2×10^{19} m^{-2}. The energy reported by the MHIMS and TESSIM simulations obviously corresponds to the second site. Considering the concentrations of the different sites reported by Markelj et al. [28], such energy would be encountered for coverage between 0.17 and 0.31 (dashed lines on figure 2a). Such coverages would be experienced at temperatures ranging from 450 K to 600 K as shown in our previous work

[16]. At lower temperature, below 450 K, the low energy desorption site can be populated and thus the coverage increases while the desorption energy decreases. Taking the value of 1.05 eV, reported by Markelj et al. [28], one gets: $E_D(\theta \approx 1) \approx 0.5$ eV. At high temperature, above 600 K, the coverage decreases and only the sites with the high desorption energy are populated. Taking the value of 2.2 eV [28], one gets: $E_D(\theta \approx 0) \approx 1.1$ eV. In the present simulation, only the low coverage part is useful with θ ranging from 0.3 to 0 since the lowest exposure temperature is 450 K.

The evolution of E_A with the coverage (figure 2b) can be obtained from the experimental depth profile and the concentration of hydrogen on the surface at steady-state. For exposure at 450 K and 600 K, the value has already been obtained from our previous simulations [16]. Values of surface energies for higher temperatures (800 K, 900 K and 1000 K) need to be determined following the method presented in [16].

In the bulk, once the steady-state between trapping and detrapping processes is reached, the concentration of trapped particles $c_{t,i}$ (m⁻³) is proportional to the concentration of traps n_i (m⁻³): $c_{t,i} = R_{trap,i}(c_m) \cdot n_i$, where $R_{trap,i}(c_m)$ is the equilibrium ratio defined by the equation (8) in [16]. For a constant temperature, it depends on the concentration of interstitial particle c_m (m⁻³) and the detrapping energy $E_{t,i}$ of the trap i. The higher c_m is, the higher $c_{t,i}$ will be. The C_D^{exp} is the measured concentration of deuterium in the bulk at a given temperature of exposure. Here, C_D^{exp} is the experimental deuterium concentration at 1 μm below the surface (figure 4). Indeed, we will see in the next section that the concentration in the near surface region is not built up during the simultaneous exposure but during the cooling phase. In the material, the concentration of deuterium is split between the mobile particles (c_m) and the trapped particles ($c_{t,i}$): $C_D^{exp} = c_m + \Sigma_i c_{t,i}$. However, in the simulations, $c_{t,i} \propto 0.01 - 0.001$ at. % while $c_m < 10^{-8}$ at. %. Thus, we can assume that $c_m \ll c_{t,i}$, which leads to $C_D^{exp} \approx \Sigma_i c_{t,i} = \Sigma_i R_{trap,i}(c_m) \cdot n_i$. One can obtain from this equation the value c_m needed to reach C_D^{exp}.

In parallel, the steady-state concentration of deuterium at the surface c_{surf} is calculated knowing the exposure temperature, the incident flux of atoms and the value of E_D presented on figure 2(a). The solid line of figure 2 is the $E_D(\theta)$ evolution put as input of the simulation and the open circles give the couples $(\theta_T, E_D(\theta_T))$ in steady state during the simultaneous exposure at the specified temperatures [16].

According to [16], c_m and c_{surf} are linked by equation 2 in steady state:

$$c_m = \frac{\nu_{sb}(T)}{\nu_{bs}(T)} \frac{c_{surf}}{1 - \theta} \tag{2}$$

Where

- $\nu_{sb}(T) \propto \exp\left(-\frac{E_A}{k_B T}\right)$, with T the temperature (K) and k_B the Boltzmann constant, is the rate constant for the absorption process from the surface to the bulk,

- $\nu_{bs} \propto \exp(-\frac{E_R}{k_B T})$ is the rate constant for the resurfacing process from the bulk to the surface.

Using this equation and using the trapping parameters (n_i, $E_{t,i}$) determined in part 4 of this paper, we are able to obtain values of E_A reported in figure 2(b) for the three temperatures 800 K, 900 K and 1000 K (open circle). They range between 1.85 eV (1000 K) and 2.01 eV (800 K) which is in a very good agreement with the data obtained by DFT calculations for low coverages [29, 30, 31, 32].

From our procedure, E_A should peak for a coverage of about 0.06 (exposure at 800 K). From our understanding, there is no obvious physical justification for such peaking. Thus, we decided to take a mean value which gives the solid line in figure 2(b): E_A is increasing when the coverage is decreasing and its maximum value is 2.00 eV.

4. Simulation results

4.1 Simulation of simultaneous W/D exposure experiments

a. Population of traps by D atoms

This section is devoted to the determination of the free trapping parameters for the simultaneous exposure experiments i.e. the detrapping energies $E_{t,i}$ and the trap concentrations n_i. Similarly to what has been done in [16], the undamaged part of the material is simulated by two intrinsic traps with detrapping energies of 0.85 eV and 1.00 eV with a trap concentrations of 0.01 at.%. In any case, as already discussed in [16], due to their low trapping energy, these two traps do not affect the TDS spectra obtained after a D atom exposure at 600 K.

The damaged layer is simulated with two traps. Their detrapping energies and trap concentrations are determined by reproducing experimental TDS spectra and NRA depth profiles. The values used in the simulations are reported in table 1. The energies reported in table 1 are the average of all the detrapping energies used in the simulations. The scattering of the detrapping energies around these averages are given by the accuracy reported in this table. Thus, it is not (directly) linked to the precision of the temperature measurement during the TDS. Figure 3 shows the comparison between the experimental and simulated deuterium depth profiles (a) and TDS spectra (b). Due to the ambiguity of the W irradiation beam diameter and shape (being more ellipse shape that round) we have difficulties to determine the absolute values of deuterium desorption signal during TDS experiments per surface area from the TDS spectra. For this reason, we will determine the detrapping energy and the relative concentration of traps by reproducing the shape and position of the peaks in the TDS spectra. The absolute amount of created traps is determined by reproducing the NRA depth profiles after the D re-exposure at 600 K.

From the NRA depth profiles a constant D concentration level in the whole damaged zone is observed. The highest D concentration is obtained for the sample simultaneously damaged and exposed to D at 450 K decreasing for higher temperatures but stabilizing for temperatures > 800 K. The TDS spectra show a single broad peak with maximum at around 800 K, decreasing for simultaneous W/D exposure at higher temperatures. There is a distinct shoulder on the right side of the peak for the 450 K, 600 K and 800 K case which disappears for the 900 K and 1000 K experiment. A similar single TDS peak was obtained in the case of sequential damaging at room temperature and exposed to D atoms at 600 K [19]. As can be seen in figure 3, the maximal concentration of deuterium in the damaged zone is reproduced within the experimental error bars by the simulation as well as the thickness of the damaged zone. However, the steps observed in the experiments between 1 μm and 2 μm is only qualitatively reproduced. One could reproduce more accurately this depth profile by complicating the distribution function f(x). However, it would add more parameters to the model. Concerning the reproduction of the TDS spectra, we quantify the difference between simulations and experiments with the relative error between the experimental desorption rate (R_{exp}) and the simulated one (R_{sim}): $\epsilon = \frac{\int |R_{exp} - R_{sim}|}{\int R_{exp}}$. For this set of simulation, with only two traps in the damaged zone, we managed to reduced ϵ below 15 % (and below 10 % for 900 K and 1000 K). Above 1100 K and below 600 K heating temperature during TDS, the experimental ground level of experiments is higher than the one of the simulation (which is close to zero). This accounts for 2-3 % in the total relative error. Considering the error outside the main part of the TDS spectra, between 600 K and 1000 K, the data in the main part are reproduced with an error below 7-12 %.
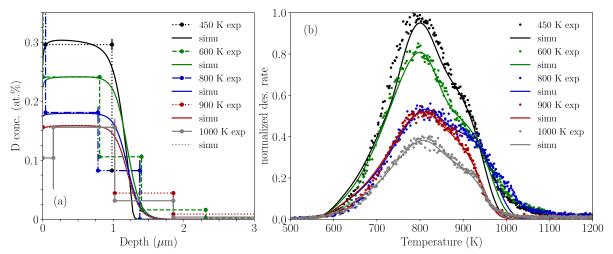

Figure 3. Comparison between the simulated and experimental NRA depth profile (a) and TDS spectra (b) obtained after the re-exposure at 600 K. The temperatures in the legends are the temperature during the simultaneous W/D exposure.

b. Simultaneous W/D exposure

The determination of trapping parameters of the model i.e. detrapping energies $E_{t,i}$ and trap concentrations n_i was shown in the previous sub-section, where the part of the simulation dedicated to

the re-exposure to D atoms at 600 K and the following TDS is presented. The trapping parameters of determined self-damaged traps are given in table 1. In this sub-section, we present the simulation results obtained after the simultaneous W/D exposure and the cooling down step (before the D re-exposure at 600 K). The trapping concentrations and energies are determined from the final depth profiles and TDS spectra after D re-exposure at 600 K (see previous sub-section). Comparison between the simulated deuterium depth profiles and the experimental depth profiles is shown in figure 4. The D concentration obtained from experiment decreases and the D penetration depth increases with the W/D exposure temperature, being 0.1 µm for 450 K, 0.7 µm at 600 K and the whole damaging zone of 1 µm for higher temperatures.

The energy barriers at the surface control the concentration of mobile deuterium. Thus, they also control the total concentration of trapped deuterium and the depth reached by deuterium [16]. The energy barrier has already been determined in our previous work [16] for temperatures of 500 K and 600 K which guarantees the good agreement between the experimental and the simulated depth profiles for exposures at 450 K and 600 K. Especially, the depth profile at 450 K, in which the deuterium atoms do not migrate deeper than 0.1 µm, is well reproduced by the simulation. For the 600 K case, the simulation overestimates the D concentration but underestimates the migration depth. In both cases, and particularly for the 450 K exposure, the damaged layer is not fully filled with deuterium after 4 h of D exposure. Low temperature decreases the diffusivity as well as the concentration of mobile particles which in turn also decreases the migration speed of deuterium toward the bulk [16, 11].

For the exposure at 800 K, the value of E_A in the simulation is lower (about 0.08 eV) than the one calculated from the obtained experimental deuterium concentration at 1 µm (solid line vs open circle in figure 2b). Thus, the concentration of deuterium at this depth in the simulation is higher than the experimental one. For the exposure at 900 K, the value of E_A in the simulation is the same as the one calculated in the previous section (figure 2b) which in turn leads to a good match between simulated and experimental concentration in the bulk. Finally, for the exposure at 1000 K, the value of E_A in the simulation is about 0.15 eV higher than the one needed to obtain the experimental deuterium concentration at 1 µm. It leads to a much lower deuterium concentration in the bulk. The overestimation of the concentration above 1 µm is due to the smooth decrease of the distribution of the created traps near the end of the damage zone. For the highest three sample temperatures (800 K, 900 K and 1000 K), the simulations reproduce well the increase of the concentration of deuterium in the first 0.1 µm which is observed experimentally. In the simulations, this increase of the concentration is explained by the 3-minutes delay between the beginning of the cooling phase and the end of the D exposure.

During these 3 minutes the exposure is still running while the temperature decreases. This leads to the following consequences: first, D atoms are additionally trapped close to the surface, since 3 minutes is a short exposure time and D atoms can only travel a small distance (few 0.1 µm).

Secondly, the concentration of mobile particle does not rapidly drop during the cooling. Close to the surface, the detrapping processes are frozen and less efficient. It follows that in the near surface area, the equilibrium ratios $(\frac{c_{t,i}}{n_i})$ increase. For the 800 K simulation, the equilibrium ratio of the most present traps (self-damaged traps 1 see table 1) is 0.16 before the cooling and it is ~1 right after the end of the D exposure. This leads to an efficient trapping of the atoms inserted during this 3-minutes period in the traps close to the surface and thus to an increase of the near surface D concentration.
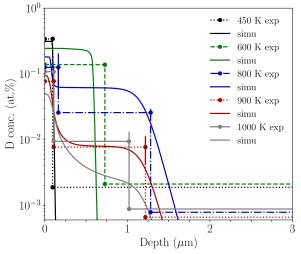

Figure 4. Comparison between the simulated and experimental D depth profiles after the simultaneous D/W exposure. The indicated temperatures refer to the temperatures during the simultaneous D/W exposure.

4.2 Simulation of sequential W-ion damaging at elevated temperatures and D-atom exposure

In this section, the free trapping parameters of the model are determined for the sequential W-ion damaging experiments at elevated temperatures and D-atom exposure, in [11] called *damaging at elevated temperatures*. Again, in addition to the two self-damaged traps, 2 intrinsic traps are added to the simulations. Since the D-atom exposure temperature in these experiments is 600 K, the intrinsic traps do not retain sufficient deuterium amount to give an apparent peak in the TDS spectra. As for the D exposure simulations, the shape of the TDS spectra and the position of the peaks give indication on the value of detrapping energies and relative trap densities while the experimental D depth profiles give the absolute values for the total concentration of traps. Figure 5 shows the comparison between experimental and simulated depth profiles (a) and TDS spectra (b). Similar to the simultaneous experiment the D depth profile is flat in the damaged zone, down to about 1 μm, and the D concentration decreases with the increase of the W-ion damaging temperature systematically. Again, the simulated depth profiles reproduce the flat absolute concentration in the damaged zone as well as the thickness of the damaged layer. The TDS spectra are similar in the case of simultaneous W/D exposure showing a single peak with a maximum at around 800 K. Also in this case the peak changes

its shape above 800 K. For this set of simulations, the relative error defined previously is about 10 % for the 300 K and 600 K cases, 15 % for the 1000 K case and 20 % for the 800 K case. Again, the difference of ground level between experimental and simulation desorption rate leads to an error of about 3 % for the 300 K, 600 K and 800 K cases and 5% for the 1000 K case. There is also the tail above around 1000 K in the experiments which is not seen in the simulations and which accounts for about 5% (300 K, 600 K and 1000 K cases) and 9 % for the 800 K (small peak at 1050 K).
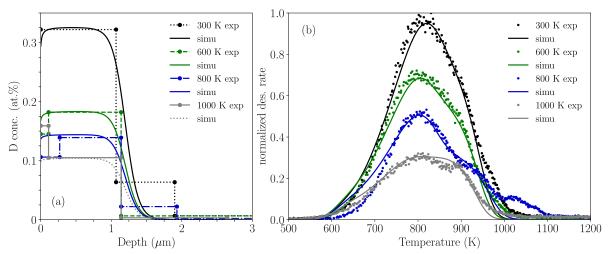

Figure 5. Comparison between the simulated and experimental NRA depth profile (a) and TDS spectra (b) obtained after exposure at 600 K for sequential W-ion damaging. The temperatures in the legends are the damaging temperature.

Damaging Temperature	Self-damaged trap 1 at.%	Self-damaged trap 2 at.%
	$E_t = 1.83 \pm 0.05$ eV	$E_t = 2.10 \pm 0.06$ eV
Simultaneous W/D exposure		
450 K	0.205	0.110
600 K	0.160	0.085
800 K	0.100	0.080
900 K	0.095	0.065
1000 K	0.100	0.060
Sequential W/D exposure		
300 K	0.210	0.120
600 K	0.110	0.070
800 K	0.095	0.050
1000 K	0.045	0.060

Table 1. Trapping parameters for the two self-damaged traps used in the simulations of simultaneous and sequential W-ion damaging and D-atom exposure. The detrapping energies E_t from the different simulations are averaged and their scattering around the average value is denoted by the accuracy in this table.

5. Discussion

In both sets of simulations, simultaneous and sequential, two self-damaged traps have been used with the same detrapping energy. The energies of these traps are the same as the one already used in our previous set of simulations [16] (1.85 eV and 2.06 eV). In the present set of simulations, we did not use the trap with de-trapping energy of 1.65 eV determined earlier. In [16], the presence of this low energy trap was mandatory in order to reproduce the isothermal desorption data at 600 K [11] and is also reported in other simulation work [19, 32]. These traps start to anneal at 500 K and it is completely annealed above 800 K for damaging with 20 MeV W ions [16]. In addition, the exposure temperature (600 K) could lead to an efficient detrapping process. Even if this trap would retain D during exposure at 450 K, it would release it during the re-exposure at 600 K. Therefore, the peak in the TDS spectra corresponding to this low energy of trapping is not visible anymore. These de-trapping energies (1.85 eV and 2.06 eV) are also in the range of those already published for various W damaging studies (with W ions [16, 19, 33, 34] and neutron [35]). In the discussion of [16] the trap with energy of 1.85 eV was attributed to dislocation loops and the highest energy trap (2.06 eV) was attributed to cavities.

The purpose of the simultaneous exposure study is to investigate the effects of the stabilization of self-damaged traps by deuterium during their creation. This has already been expressed by looking at the maximum experimental concentration of retained deuterium as function of the damaging temperature [11]. As already pointed out in [11], the simultaneous D/W exposure leads to a higher trap concentration compared to the sequential exposures. Thus, it is concluded that the presence of D in the metals during the damaging prevents the defects to anneal. This effect seems to be especially pronounced at high temperature (900 K and 1000 K). From the simulations, one can gain information on the total concentration of traps used to simulate the experimental results as well as the maximum concentration of mobile particles c_m during the simultaneous exposures. This quantity is particularly important since it might be the quantity driving the trap stabilizations. These two quantities are plotted on figure 6.
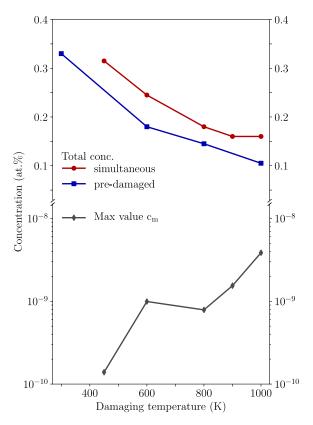
Figure 6. Evolution of the total self-damaged trap concentration assuming occupancy one as function of the damaging temperature for both simultaneous and pre-damaged materials (top) and evolution of the maximum concentration of mobile particles c_m (bottom) with the exposure temperature (simultaneous exposure only). The top scale is linear and the bottom scale is logarithmic.

For D ion implantations, c_m is directly proportional to the incident flux of ions and inversely proportional to the diffusion coefficient: for a constant ion flux, c_m will decrease as a function of the temperature as the diffusion coefficient increases. In these simulations, even though c_m decreases between 600 K and 800 K, the opposite trend is observed for c_m (figure 6). This behavior looks similar to the one as a Sievert's law that would drive the concentration of the interstitial hydrogen for gas/H_2 exposure. Indeed, in both cases, the kinetic limiting processes are the ones occurring at the surface. The decrease of c_m between 600 K and 800 K is only due to the increase of E_A between this two temperatures. It has to be noted that, if one would have use the E_A values given by the open circle of figure 2b, the c_m value at 800 K would have been lower, being 1.6×10^{-10} at.% instead of 8×10^{-10} at.%. This increase of interstitial particles at higher temperatures can explain the large effect of the trap stabilization at high temperature (900 K – 1000 K) which is observed in figure 6 on the evolution of the total concentration of self-damaged traps. Again, if one would have taken the value of E_A given by the open circle in figure 2b, the c_m value at 1000 K would have been higher, being 2.9×10^{-8} at.% instead of 3.9×10^{-9} at.%.

With the help of the simulations, we can also go further and address the effect of deuterium on trap stabilization, trap by trap. To do that, the evolution of the trap concentration obtained from the

16

simulation is plotted as function of the damaging temperature in figure 7 for the self-damaged trap 1 (a) and trap 2 (b).
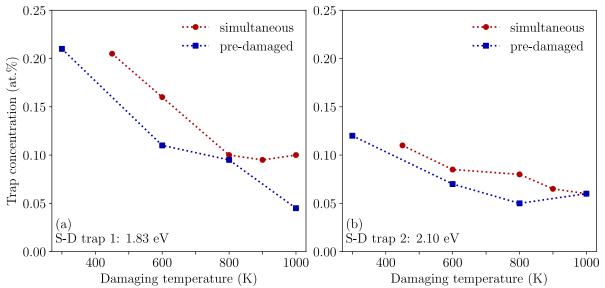

Figure 7. Comparison of trap concentrations used in the simulation of simultaneous and sequential W-ion damaging and D-atom exposure for the self-damaged trap 1 (a) and trap 2 (b).

For all damaging temperatures, the self-damaged trap 1 ($E_t = 1.83$ eV) has significantly higher concentrations while exposing simultaneously D atoms and W ions, except for a damaging temperature of 800 K. It shows that the presence of D atoms during the damaging prevents a complete annihilation of the traps while rising the temperature. The fact that few differences are observed for the 800 K might come from the low c_m during the exposure at this temperature (figure 6). The trap stabilization is especially clear for the two highest temperatures. Indeed, between 800 K and 1000 K, if no D atoms are present to stabilize the traps, they are progressively annealed as the temperature rises up. In the case of simultaneous W/D exposure stabilization of traps is observed in this temperature range. To check the reproducibility of this high temperature effect, simultaneous W/D exposure was repeated at 1000 K and tested for even higher temperature of 1130 K. With the additional experiments performed, this effect of stabilization was confirmed, not showing decrease of maximum D atom concentration above 900 K. Namely, the maximum D concentrations obtained were 0.17 ± 0.01 at. % at 1000 K and 0.16 ± 0.01 at. % at 1130 K what is similar to the previous experiment [11] where 0.155 at.% was obtained for 900 K and 1000 K. This shows that the insertion of D atoms during the damaging prevents the annealing of these traps. The stabilization of self-damaged trap 2 ($E_t = 2.10$ eV) can be observed on figure 7(b). This time, it seems that stabilization appears mostly in the low temperature range and is especially pronounced at 800 K. Previous simulations shows that the concentration of this trap increases at high temperature while annealing the damaged samples before the D exposure [16]. This increase can be also observed for sample damaged at different temperature on figure 7(b) for the sequential case. It has been related to the growth of the vacancy cluster to which

this trap is assigned [16]. The presence of the D interstitial atom that can feed the vacancy clusters can slow down the growth mechanism by increasing the migration barrier of the vacancies [22] and by extension of the vacancy clusters. Thus, during the simultaneous exposure, the high concentration of mobile D particles might spoil this growth preventing the concentration of self-damaged trap #2 to increase from 800 K to 1000 K (figure 7(b)) as is the case for the pre-damaged case.

6. Conclusion

The effect of the presence of hydrogen isotope on defect evolution was studied by performing damaging of W samples by 10.8 MeV W ions at elevated temperatures with and without D-atom exposure during the damaging process. In order to determine the concentration of traps inside the material the samples were additionally exposed to D atoms at 600 K. The atoms populate the defects created during the damaging without creating any additional damage. The D depth profile, the total deuterium amount and detrapping properties for each individual sample were obtained utilizing NRA and TDS methods. By modeling D depth profile and D desorption spectra by the MHIMS code we could determine the detrapping energies and trap concentration for different sample temperatures for the two experiments: sequential and simultaneous W/D exposure. In order to model the simultaneous experiment a model of trap creation during the D-atom exposure was implemented into the MHIMS code. This gave us also the possibility to simulate the D depth profiles measured after the four hours of simultaneous W-ion damaging and D-atom exposure and the agreement between the experiment and the measurement was good especially concerning the penetration depths. Namely, in the case of 450 K sample temperature the atoms penetrated only 0.1 μm, at 600 K 0.7 μm and above 800 K the whole damaging area of 1 μm is populated by D atoms. Namely, the energy barriers at the surface control the concentration of mobile deuterium. Thus, they also control the total concentration of trapped deuterium and the depth reached by deuterium. Thanks to the surface model we could also determine the energy barrier for the HI atoms to migrate from the surface into the bulk. It is shown that there is a temperature dependence of the migration barrier which at high temperatures and low hydrogen atom coverages stabilizes at 2 eV. This value is in good agreement with the DFT calculations [29, 30, 31, 32]. This gives also the explanation for the discrepancy between the migration barrier as obtained in our previous studied preformed with D atoms [16, 19], as compared to DFT calculations and the Fraunfelder experiment performed with gas loading [37] to which theoretical results are compared. The Fraunfelder experiment was performed at high temperatures from 1120 K to 2080 K, therefore at low surface coverages since the molecules cannot penetrate into bulk at lower temperatures due to the high surface barrier what is not the case of our 0.28 eV D atoms that can migrate into bulk above 500 K as was shown in [19].

The comparison of traps concentrations for simultaneous and sequential samples exposed to D atoms at the same temperature of 600 K gives us direct evidence on the effect of presence of mobile D on trap evolution. This was directly evaluated in this paper. We believe that this effect is not specific on the hydrogen isotope used and can be used for extrapolation to tritium. The first trap with 1.83 eV detrapping energy being attributed to dislocation loops is higher for simultaneous experiment at all temperatures whereas the 2.10 eV trap is less affected by the experimental procedure and presence of HI.

The stabilization of traps induced by the presence of hydrogen evidenced here might have an important effect on the total amount of tritium that a W divertor target can accommodate during ITER operation. Recent simulations predict that the tritium retention in W divertor target is higher in neutron-damaged material than in material not damaged by neutrons [4]. The ratio damaged/undamaged is about 1 in the area where the temperature below 450 K but it can reach 30 in the hotter area where the temperature can reach 1000 K or more. Thus, the stabilization of the traps presented in this paper, that was not taken into account in the tokamak cycle simulations presented in [4], will enhance the retention in damaged W especially at the strike point position where the temperature is the highest (and so, where the stabilization is the most efficient according to the present data).

The experiment presented in this paper was performed by D atoms where the way to obtain the information about trap concentration was indirect by populating the defects by D atoms at 600 K. There is a about factor of 1.3-1.5 increase in D atom concentration when comparing the D retention for simultaneous and sequential experiment over the whole studied temperature range. This means that even when at the ITER or DEMO relevant temperatures of around 1000 K – 1300 K near the strike points there will be this difference of HI retention due to the presence of hydrogen. However, the HI fluxes of ions and neutrals to the walls of reactor will be few orders of magnitude higher (10^{21}-10^{24} particles/cm^{2}s) as compared to the present study (5.4×10^{18} D/m^{2}s). This will increase the concentration of mobile HI atoms in the bulk of material. How increase of concentration the mobile particles influences on the stabilization of traps is not known. In this paper we have made the first step, showing that there is an effect. Further studies are needed where the flux of atoms or ions has to be increased to see whether HI flux has some influence and how this influences on the defect creation and total retention.

References

[1] V. Chan, R. Stambaugh, A. Garofalo, J. Canik, J. Kinsey and et al., "A fusion development facility on the critical path to fusion energy," *Nuc. Fusion,* vol. 51, no. 8, p. 083019, 2011.

[2] J. Roth, E. Tsitrone, A. Loarte, T. Loarer, R. Neu, V. Philipps and S. Brezinsek, "Recent analysis of key plasma wall interactions issues for ITER," *Journal of Nuclear Materials,* vol. 390–391, no. 1., p. 1–9, 2009.

[3] J.-H.You, "A review on two previous divertor target concepts for DEMO: mutual impact between structural design requirements and materials performance," *Nucl. Fusion,* vol. 55, p. 113026, 2015.

[4] E. A. Hodille, E. Bernard, S. Markelj, J. Mougenot, C. S. Becquart, R. Bisson and C. Grisolia, "Estimation of the tritium retention in ITER tungsten divertor target using macroscopic rate equations simulations," *Phys. Scr. ,* vol. T170, p. 014033, 2017.

[5] B. Wirth, K. Nordlung, D. Whyte and D. Xu, "Fusion materials modeling: Challenges and opportunities," *MRS Bulletin,* vol. 36, p. 216–222, 2011.

[6] J. Marian and e. al, "Recent advances in modeling and simulation of the exposure and response of tungsten to fusion energy conditions," *Nucl. Fusion,* vol. 57, p. 092008, 2017.

[7] W. R. Wampler and R. P. Doerner, "The influence of displacement damage on deuterium retention in tungsten exposed to plasma," *Nuclear Fusion,* vol. 49, p. 115023, 2009.

[8] Y. Hatano, M. Shimada, T. Otsuka, Y. Oya and V. K. Alimov, "Deuterium trapping at defects created with neutron and ion irradiations in tungsten," *Nuclear Fusion,* vol. 53, p. 073006, 2013.

[9] O. V. Ogorodnikova, Y. Gasparyan, V. Efimov, Ł. Ciupiński and J. Grzonka, "Annealing of radiation-induced damage in tungsten under and after irradiation with 20 MeV self-ions," *Journal of Nuclear Materials,* vol. 451, no. 1-3, pp. 379-386, 2014.

[10] O. V. Ogorodnikova and V. Gann, "Simulation of neutron-induced damage in tungsten by irradiation with energetic self-ions," *Journal of Nuclear Materials,* vol. 460, p. 60, 2015.

[11] S. Markelj, T. Schwarz_Selinger, A. Zaloznik, M. Kelemen, P. Vavpetic, P. Pelicon, E. Hodille and C. Grisolia, "Deuterium retention in tungsten simultaneously damaged by high energy W ions and loaded by D atoms," *Nucl. Mater. Energ.,* vol. 12, pp. 169-174, 2017.

[12] S. Markelj, A. Založnik, T. Schwarz-Selinger, O. V. Ogorodnikova, P. Vavpetič, P. Pelicon and I. Čadež, "In situ NRA study of hydrogen isotope exchange in self-ion damaged tungsten exposed to neutral atoms," *Journal of Nuclear Materials,* vol. 469, p. 133–144, 2016.

[13] A. Založnik, S. Markelj, T. Schwarz-Selinger, Ł. Ciupiński, J. Grzonka, V. P. and P. Pelicon, "The influence of the annealing temperature on deuterium retention in self-damaged tungsten," *Phys. Scr.,* vol. T167, p. 014031, 2016.

[14] P. Wang, W. Jacob, L. Gao, T. Dürbeck and T. Schwarz-Selinger, "Comparing deuterium retention in tungsten films measured by temperature programmed desorption and nuclear reaction analysis," *Nuclear Instruments and Methods in Physics Research Section B: Beam Interactions with Materials and Atoms,* vol. 300, p. 54–61, 2013.

[15] E. A. Hodille, X. Bonnin, R. Bisson, T. Angot, C. S. Becquart, J.-M. Layet and C. Grisolia,

"Macroscopic rate equation modeling of trapping/detrapping of hydrogen isotopes in tungsten materials," *J. Nucl. Mater. ,* vol. 467, pp. 424-431, 2015.

[16] E. A. Hodille, A. Založnik, S. Markelj, T. Schwarz-Selinger, C. S. Becquart, R. Bisson and C. Grisolia, "Simulations of atomic deuterium exposure in self-damaged tungsten," *Nucl. Fusion,* vol. 57, p. 056002, 2017.

[17] G. R. Longhurst, "TMAP-7 user manual," Edaho National Laboratory Report, INEEL.EXT-04-2004, 2004.

[18] K. Schmid, V. Rieger and A. Manhard, "Comparison of hydrogen retention in W and W/Ta alloys," *J. Nucl. Mater. ,* vol. 426, pp. 247-253, 2012.

[19] A. Zaloznik, S. Markelj, T. Schwarz-Selinger and K. Schmid, "Deuterium atom loading of self-damaged tungsten at different sample temperatures," *J. Nucl. Mater.,* vol. 496, pp. 1-8, 2017.

[20] O. V. Ogorodnikova, J. Roth and M. Mayer, "Deuterium retention in tungsten in dependence of the surface conditions," *J. Nucl. Mater. ,* Vols. 313-316, pp. 469-477, 2003.

[21] M. H. J. 't Hoen, B. Tyburska-Püschel, K. Ertl, M. Mayer, J. Rapp, A. W. Kleyn and P. A. Zeijmans van Emmichoven, "Saturation of deuterium retention in self-damaged tungsten exposed to high-flux plasmas," *Nucl. fusion 52,* p. 023008, 2012.

[22] V. Alimov, Y. Hatano, B. Tyburska-Püschel, K. Sugiyama, I. Takagi, Y. Furuta, J. Dorner, M. Fußeder, K. Isobe, T. Yamanishi and M. Matsuyama, "Deuterium retention in tungsten damaged with W ions to various damage levels," *Journal of Nuclear Materials,* vol. 441, p. 280–285, 2013.

[23] N. Fernandez, Y. Ferro and D. Kato, "Hydrogen diffusion and vacancies formation in tungsten: Density Functional Theory calculations and statistical models," *Acta Mater. ,* vol. 94, pp. 307-318, 2015.

[24] A. Nojima and K. Yamashita, "A theoretical study of hydrogen adsorption and diffusion on a W(110) surface," *Surf. Sci. ,* vol. 601, pp. 3003-3011, 2007.

[25] Z. A. Piazza, M. Ajmalghan, Y. Ferro and R. D. Kolasinski, "Saturation of tungsten surfaces with hydrogen: A density functional theory study complemented by low energy ion scattering and direct recoil spectroscopy data," *Acta Mater.,* vol. 145, pp. 388-398, 2018.

[26] P. W. Tamm and L. D. Schmidt, "Binding States of hydrogen on tungsten," *J. Chem. Phys. ,* vol. 54, p. 4775, 1971.

[27] T.-U. Nahm and R. Gomer, "The adsorption of hydrogen on W(110) and Fe covered by W(110)," *Surf. Sci. ,* vol. 375, pp. 281-292, 1997.

[28] S. Markelj, O. V. Ogorodnikova, P. Pelicon, T. Schwarz-Selinger and I. Cadez, "Temperature dependence of D atom adsorption on polycrystalline tungsten," *Appl. Surf. Sci. ,* vol. 282, pp. 478-486, 2013.

[29] K. Heinola and T. Ahlgren, "First-principles study of H on the reconstructed W(100) surface," *Phys. Rev. B ,* vol. 81, p. 073409, 2010.

[30] D. F. Johnson and E. A. Carter, "Hydrogen in tungsten: Absorption, diffusion, vacancy trapping, and decohesion," *J. Mater. Res.,* vol. 25, no. 2, p. 315, 2010.

[31] A. Moitra and K. Solanki, "Adsorption and penetration of hydrogen in W: A first principles study," *Comp. Mater. Sci. ,* vol. 50, pp. 2291-2294, 2011.

[32] P. Ferrin, S. Kandoi, A. Udaykumar Nilekar and M. Mavrikakis, "Hydrogen adsorption and diffusion on and in transition metal surfaces: A DFT study," *Surf. Sci. ,* vol. 606, pp. 679-689, 2012.

[33] Y. M. Gasparyan, O. V. Ogorodnikova, V. S. Efimov, A. Mednikov, E. D. Marenkov, A. A. Pisarev, S. Markelj and I. Cadez, "Thermal desorption from self-damaged tungsten exposed to deuterium atoms," *J. Nucl. Mater. ,* vol. 463, pp. 1013-1016, 2015.

[34] O. V. Ogorodnikova, "Fundamental aspects of deuterium retention in tungsten at high flux

plasma exposure," *J. Appl. Phys. ,* vol. 118, p. 074902, 2015.

[35] M. 't Hoen, M. Mayer, A. Kleyn, H. Schut and P. Zeijlmans van Emmichoven, "Reduced deuterium retention in self-damaged tungsten exposed to high-flux plasmas at high surface temperatures," *Nucl. Fusion,* vol. 53, p. 043003, 2013.

[36] M. Shimada, G. Gao, Y. Hatano, T. Oya, M. Hara and P. Calderoni, "The deuterium depth profile in neutron-irradiated tungsten exposed to plasma," *Phys. Scr. T 145,* p. 014051, 2011.

[37] Fraunfelder, " Solution and Diffusion of Hydrogen in Tungsten," *Journal of vacuum Science and Technology,* vol. 6, p. 388, 1968.